ELSEVIER

Biochimica et Biophysica Acta 1325 (1997) 329–342

BIOCHIMICA ET BIOPHYSICA ACTA
BBA

In vitro study of passive nitrate transport by native and reconstituted plasma membrane vesicles from corn root cells

J.-P. Grouzis *, P. Pouliquin [1], J. Rigaud, C. Grignon, R. Gibrat

Biochimie et Physiologie Moléculaire des Plantes, CNRS (URA 2133) / INRA / ENSA-M, Place Viala, F-34060 Montpellier, Cedex 1, France

Received 30 September 1996; revised 11 December 1996; accepted 12 December 1996

Abstract

Proteins from phase-partitioned corn root plasma membrane were reconstituted into soybean lipids/egg PC (8:2, w:w) using deoxycholate and rapid gel filtration to eliminate the detergent. All (H^+)ATPase molecules were inside-out reinserted and the initial activity was totally recovered in an homogeneous vesicle preparation. In addition, membrane tightness greatly increased, as shown by the size and stability of the response of the fluorescent membrane potential probe (oxonol VI) to an imposed K^+ diffusion gradient. Consequently, the H^+-pumping activity of the (H^+)ATPase, monitored with the fluorescent pH probe (ACMA), increased 20-fold after reconstitution. A protein-mediated passive transport of nitrate was first demonstrated by the ability of NO_3^- to electrically short-circuit the (H^+)ATPase in plasma membrane vesicles and not in liposomes containing only the purified enzyme. The passive transport was saturable ($K_m \approx 5$ mM), thermolabile, inhibited by the arginine reagent phenylglyoxal, and selective ($NO_3^- > I^- \approx ClO_3^- \approx Br^- > Cl^- \approx NO_2^- >$ Iminodiacetate $\approx SO_4^{2-}$). Passive NO_3^- transport was also determined, independently of the (H^+)ATPase, from the NO_3^--dependent augmentation of the dissipation rate of imposed diffusion potentials. This second transport assay gave similar K_m for NO_3^- and should be suitable to continue the functional and biochemical characterization of the NO_3^- transport system.

Keywords: Plant plasma membrane; (H^+)ATPase; Membrane vesicle; Protein reconstitution; Passive nitrate transport; Transmembrane pH and electrical potential gradient; 9-Amino-6-chloro-2-methoxyacridine; Oxonol VI; Corn root; (*Zea mays* L.)

1. Introduction

Nitrate uptake and reduction by plants is a major N input in terrestrial trophic chains. From in vivo uptake studies, a variety of carriers is predicted to mediate NO_3^- transport at the plant root plasma membrane: one class comprises constitutive and inducible active uptake systems which operate as nH^+: mNO_3^- symporters with $n > m$ and with a high, or a low affinity for NO_3^- [1]. Another class comprises passive systems responsible for a NO_3^- efflux from the cells. NO_3^- efflux regulates the rate of its net uptake [2,3], although the maximum value of the

Abbreviations: ACMA, 9-amino-6-chloro-2-methoxyacridine; A-9-C, anthracen-9-carboxylic acid; AE, ethacrynic acid; BSA, bovine serum albumin; BTP, 1,3-bis(tris(hydroxymethyl)-methylamino)propane; CMC, critical micellar concentration; DEPC, diethyl pyrocarbonate; DIDS, stilben 4, 4′-diisothiocyano-2, 2′-disulfonic acid; DOC, sodium deoxycholate; DTT, dithiothreitol; ETH, eth 149 (Li^+ ionophore); FCCP, carbonyl cyanide 4-trifluoromethoxyphenylhydrazone; IDA, iminodiacetate; NPPB, 5-nitro-2-(3-phenylpropylamino)-benzoic acid; oxonol, oxonol VI; PC, phosphatidylcholine; PGO, phenylglyoxal; R_e, effective ratio

* Corresponding author. Fax: (33) 467 525737. E-mail: grouzis@ensam.inra.fr

[1] Present address: Abteilung für Angewandte Physiologie, Ulm Universität, D-89069 Ulm, Germany.

PII S0005-2736(96)00256-8

latter mainly depends on influx [4]. Passive efflux from root cells should be also involved in NO_3^- loading of xylem vessels which conduct NO_3^- in the shoots [5]. By comparison to NO_3^- influx, NO_3^- efflux is poorly documented in spite of its physiological importance.

Use of inside-out membrane vesicles makes accessible from the controlled external medium the cytoplasmic transport site of systems mediating ion efflux in situ, facilitating their functional characterization. The major difficulty arises from the lack of a convenient method to assay NO_3^- transport across membrane vesicles. The radioisotope $^{36}ClO_3^-$ has been used as an analogue of NO_3^- to measure NO_3^- transport across isolated plasma membrane vesicles [6], but the validity of this method remains controversial [7]. In the present study, we describe two transport assays which authorize a semi-quantitative analysis of passive NO_3^- efflux. The first one makes use of the (H^+)ATPase to drive passive NO_3^- transport. The second one makes use of an imposed K^+-valinomycin diffusion potential to drive passive NO_3^- transport.

A method has been developed to reconstitute the whole plasma membrane protein content into fresh lipids to obtain an homogeneous preparation of highly tight vesicles required by these NO_3^- transport assays.

2. Materials and methods

2.1. Membrane preparation and purification of the (H^+)ATPase

Corn seeds (*Zea mays* L., var Mona) were grown as described previously [8]. Microsomes were prepared according to De Michelis and Spanswick [9]. Plasma membrane was further purified by phase partitioning according to Galtier et al. [10]. (H^+)ATPase was purified on a glycerol gradient from plasma membrane isolated on sucrose gradient [11].

2.2. Reconstitution procedure

Purified (H^+)ATPase was reconstituted in fresh lipids as described previously [12]. The reconstitution of the whole protein content of native membranes was done according to Brauer et al. [13] with the following modifications. Experiments were performed with mixed soybean phospholipids (L-α-phosphatidylcholine, type II-S, Sigma) complemented with egg phosphatidylcholine (type XVI-E, Sigma) at a ratio 8/2 (w/w) in reconstitution buffers containing 10 mM BTP-SO_4 (pH 7.5), 50 mM K_2SO_4 or Li_2SO_4 (when indicated) and 20% (v/v) glycerol or not (when indicated). Reconstitutions for experiments with K^+-valinomycin imposed diffusion gradients were performed in 1 mM Hepes-Li (pH 7.5), 50 mM Li_2SO_4, 0.5 mM K_2SO_4, 20% (v/v) glycerol. Forty mg of phospholipid were dispersed by vigorous mixing on a vortex mixer in the presence of glass beads in 1 ml reconstitution buffer, for 15 min under argon. The liposomes suspension was clarified by sonication for 15 min under argon in a Bransonic bath sonicator. The solubilization of liposomes by deoxycholate (DOC) was monitored by measuring the decrease of the turbidity of liposomes in the resuspension buffer described below, as a function of detergent concentration (data not shown). Liposomes were fully solubilized at an effective ratio $R_e = [(\text{detergent}) - \text{CMC}]/(\text{phospholipid}) = 0.6$, where CMC is the critical micellar concentration.

Plasma membrane proteins (0.8 mg in 0.7 ml of resuspension buffer containing 2 mM BTP-Cl (pH 7.2), 0.25 M sucrose, 20% (v/v) glycerol and 2 mM DTT) were mixed with 12 mg of sonicated phospholipid unless otherwise indicated. To this mixture, DOC was added such that the final concentration corresponded to a R_e of 0.6. The solubilized membranes were applied to the top of a Sephadex G-150 column (20 cm $\times$ 1.5 cm) equilibrated with reconstitution buffer and then eluted at 0.6 ml. min^{-1}. The cloudy void volume fraction (6 ml) was collected and stored in liquid N_2.

When protein dilution during chromatography was to be avoided, reconstitution was made in Sephadex G-50 minicolumns. Disposable syringes (2.5 ml) fitted with porous glass filters were filled with 1.5 ml Sephadex G-50 equilibrated with reconstitution buffer. The syringes were inserted into plastic tubes and centrifuged for 5 min at 180 $\times$ g to release extra buffer. Aliquots (220 μl) of the protein-lipid-detergent mixture, prepared as described above, were applied to the columns and centrifuged again. The volumes recovered were within 90% to 100% of the volumes applied. Proteins and lipids were totally

recovered in the cloudy void volume after Sephadex chromatography (data not shown).

2.3. Plasma membrane (H^+)ATPase hydrolytic activity

The hydrolytic activity of the plasma membrane (H^+)ATPase was determined measuring the release of P_i according to the method of Ames [14]. SDS (0.75%, w/v) was added to solubilize membranes and to prevent interferences when surfactants were used to permeabilize the vesicles. The standard incubation medium (0.5 ml final volume) contained 30 mM BTP-NO_3 (pH 6.5), 50 mM KCl, 3 mM ATP-BTP, 2 μM gramicidin to dissipate the electrochemical H^+ gradient, 1 mM Na-molybdate, 1 mM NaN_3, in the presence or in the absence of 1 mM vanadate, and membrane proteins (5 μg). The reaction was started by addition of 3 mM $MgSO_4$ (final concentration), and allowed to proceed for 30 min at 30°C.

The total (H^+)ATPase activity (from both inside-out and right side-out vesicles) was determined by adding 0.015% (w/v) Triton X-100 in the assay medium [15], or by treating the membrane with SDS according to Palmgren and Sommarin [16]. Briefly, native or reconstituted vesicles (180 $\mu g \cdot ml^{-1}$) from KI-washed microsomes and phase-partitioned plasma membranes were incubated with SDS at the indicated concentrations in 10 mM BTP-Cl (pH 6.5), 3 mM ATP-BTP, 1 mM EDTA-BTP and 1 mM DTT. After incubation for 20 min at 20°C, aliquots of 25 μl were transferred to the ATPase assay medium (0.5 ml) containing 10 mM BTP-Cl (pH 6.5), 3 mM ATP-BTP, 3 mM $MgSO_4$, 1 mM EDTA-BTP, 1 mM DTT and 50 mM KCl.

2.4. Detection of transmembrane H^+ electrochemical gradient using fluorescent probes

Fluorescence intensity of the transmembrane pH probe ACMA and the membrane potential oxonol VI probe was measured with an Aminco-Bowman Serie 2 spectrofluorometer (AB2), fitted with a stirred cuvette (2 ml of assay medium) maintained at 30°C. The excitation/emission wavelengths were 420/485 nm for ACMA and 614/646 nm for oxonol VI, respectively. In double labelling experiments, these two couples of excitation/emission wavelengths were alternatively selected during brief cycles [17]. Rates of variation of the fluorescence signals were determined from the derivation of the kinetics, using the AB2-software.

H^+-pumping activity of plasma membrane (H^+)ATPase. The H^+-pumping activity of the (H^+)ATPase was assimilated to the initial rate of fluorescence quenching of 1 μM ACMA in an assay

Table 1
Specific activity of plasma membrane (H^+)ATPase in native and reconstituted vesicles from microsomes or plasma membrane fractions purified on sucrose gradient or by phase-partition

Fractions	Hydrolytic activity [a]		Orientation [b]	V_H+ [c]	V_H+/V_{ATP}
	basal	total			
Microsomes					
native	0.23	0.70	33	1.2	5.2
reconstituted	0.70	0.70	100	5.3	7.6
	0.40 [d]	0.41 [d]	98 [d]	1.2 [d]	3.0 [d]
Plasma membrane					
Sucrose gradient					
native	0.32	0.92	35	0.7	2.2
reconstituted	0.88	0.82	107	6.0	6.8
Phase-partition					
native	0.20	1.25	16	0.3	1.5
reconstituted	1.30	1.25	103	5.8	4.5

ATP hydrolysis and H^+-pumping activities were performed on native vesicles and after reconstitution, in the absence of glycerol [d], or in the presence of 20% glycerol (v/v), as described in Section 2. The specific activities were presented as [a] nmol ATP hydrolysed $\cdot min^{-1} \cdot \mu g^{-1}$ protein, [c] % quenching $\cdot min^{-1} \cdot \mu g^{-1}$ protein (V_H+). The basal hydrolytic activity (V_{ATP}) was measured in the absence of permeabilizing agent, and the total activity was measured in the presence of 0.015% (w/v) Triton X-100. The ratio of the basal to the total activities gave the proportion of inside-out plasma membrane vesicles (H^+)ATPase, expressed in % [b].

buffer (see below) containing 1 mM ATP-BTP and 5 to 20 $\mu g \cdot ml^{-1}$ membrane protein (native or reconstituted plasma membrane vesicles) or 0.1 $\mu g \cdot ml^{-1}$ protein (liposomes only containing the glycerol gradient purified (H^+)ATPase). After incubation for 10 min at 30°C, quenching reaction was initiated by adding 2 mM $MgSO_4$. The initial rate of quenching was linear with protein concentration (data not shown) and could be expressed in specific unit (% quenching $\cdot min^{-1} \cdot \mu g^{-1}$ protein). In experiments presented in Table 1 and Fig. 1A, the assay buffer contained 30 mM BTP-Cl (pH 6.5), 30 mM BTP-NO_3 (pH 6.5), 50 mM KCl, 50 mM KBr and 100 nM valinomycin. In other experiments, the assay buffer contained 60 mM BTP-SO_4 (pH 6.5), 50 mM K_2SO_4 or K_2SO_4 plus KNO_3 at the indicated concentration (100 mM K^+).

Membrane potential. The fluorescent anion oxonol VI (50 nM) was used to probe the membrane potential, positive inside, generated by the (H^+)ATPase or inward K^+-valinomycin diffusion gradients. Fluorescence was expressed as the ratio of fluorescence augmentation in response to membrane polarisation (ΔF) to basal fluorescence at zero membrane potential (F_0). (H^+)ATPase-dependent membrane potential was generated by adding 2 mM $MgSO_4$ in an assay medium containing 10 μg proteins and 1 mM ATP-BTP, 60 mM BTP-SO_4 (pH 6.5), 50 mM K_2SO_4 or K_2SO_4 plus KNO_3 at the indicated concentration (100 mM K^+). Diffusion potential was imposed by adding K_2SO_4 or K_2SO_4 plus KNO_3 at the indicated concentration (100 mM K^+) to the assay medium containing 3.4 $\mu g \cdot ml^{-1}$ proteins, 20 nM valinomycin and 1 mM Hepes-Li (pH 6.5), 50 mM Li_2SO_4 and 0.5 mM K_2SO_4.

2.5. Protein determination

Proteins were determined according to Schaffner and Weissmann [18], with BSA as standard.

2.6. Statistics

Values in figures and tables are given as the mean ± S.E. of at least three independent experiments, unless otherwise indicated.

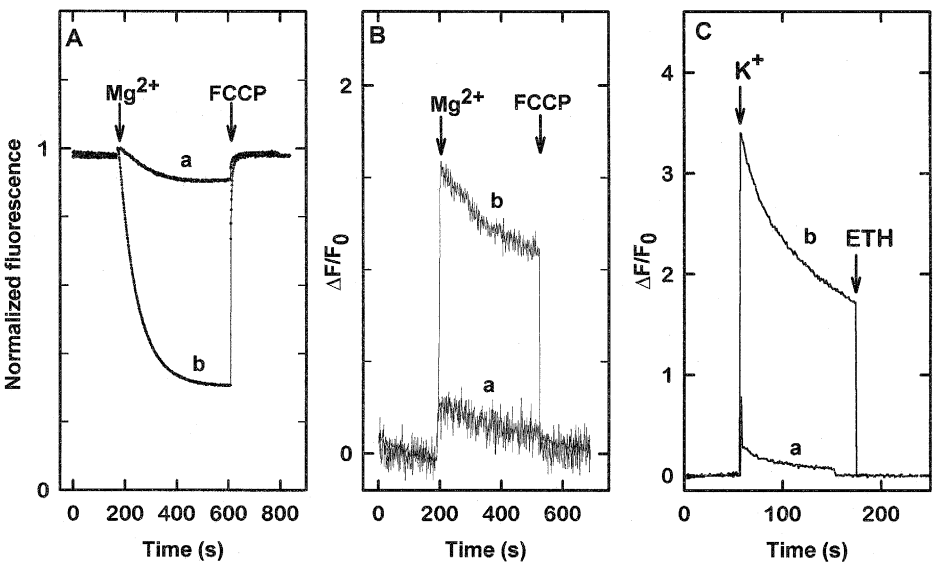

Fig. 1. Response of fluorescent probes to transmembrane pH and electrical potential gradients generated across native and reconstituted plasma membrane vesicles. The reconstitution of plasma membrane proteins in soybean lipids and the fluorescent assays were performed as described in Section 2. The vesicle acidification and the membrane potential after the (H^+)ATPase energization were detected with ACMA (A) and oxonol (B) probes, respectively. Assays were performed on native (a) and reconstituted (b) vesicles on an equal protein basis (10 μg protein in the assay cuvette). FCCP (200 nM) was added to dissipate the pH and electrical gradients at the indicated times. In C, membrane potential was created by adding 100 mM K^+ as SO_4^{2-} salt to the outside of native (a) or reconstituted (b) membrane vesicles containing 50 mM Li_2SO_4 and 0.5 mM K_2SO_4, in the presence of valinomycin (20 nM). The Li^+ ionophore ETH (200 nM) was added to collapse the membrane potential.

3. Results and analysis

3.1. Ion electrochemical gradient across native and reconstituted plasma membrane vesicles

Typical records of the H^+ electrochemical gradient generated by the plasma membrane (H^+)ATPase across native membrane vesicles are shown in Fig. 1A and B (traces a). Reconstitution of plasma membrane proteins in a mixture of soybean lipids/egg PC (8:2, w/w) at a lipid-to-protein ratio R = 15 (w/w), resulted in strongly enhanced H^+-gradient and membrane potential, as compared to native vesicles (Fig. 1A and B, traces b). This response could result from an improvement of the membrane tightness. Indeed, the size and stability of the signal emitted by the membrane potential probe after imposition of an inward K^+ diffusion gradient in the presence of valinomycin strongly increased after plasma membrane protein reconstitution (Fig. 1C), suggesting a lower membrane tightness of native vesicles.

Increasing the lipid-to-protein ratio from 2 to 30 resulted in a 'saturation-like' effect of the response of the two dyes (Fig. 2), whereas a linear correlation was observed between their responses (Fig. 2, inset). In the following, vesicles were reconstituted at R = 15.

The increase of both H^+-gradient and membrane potential created by the (H^+)ATPase (Fig. 1A and B) could also result from an augmentation of inside-out oriented pump molecules in reconstituted vesicles. The total plasma membrane (H^+)ATPase hydrolytic activity, ie the basal activity from catalytic sites on the outside of the vesicles plus the latent activity from interior-facing catalytic sites, was determined using Triton X-100 to permeabilize the vesicles [19]. The plasma membrane (H^+)ATPase latency in microsomes indicated that about 30–35% of vesicles were inside-out oriented, whereas only 16% of inside-out vesicles were present after phase-partitioning (Table 1). In both cases, reconstitution completely eliminated the latency, and the total hydrolytic activities of the plasma membrane (H^+)ATPase were the same in both native and reconstituted vesicles. When glycerol (20%, v/v) was omitted during reconstitution, Triton X-100 failed again to reveal any latent activity, but the total activity was 40% lower in proteoliposomes than in native microsomes (Table 1).

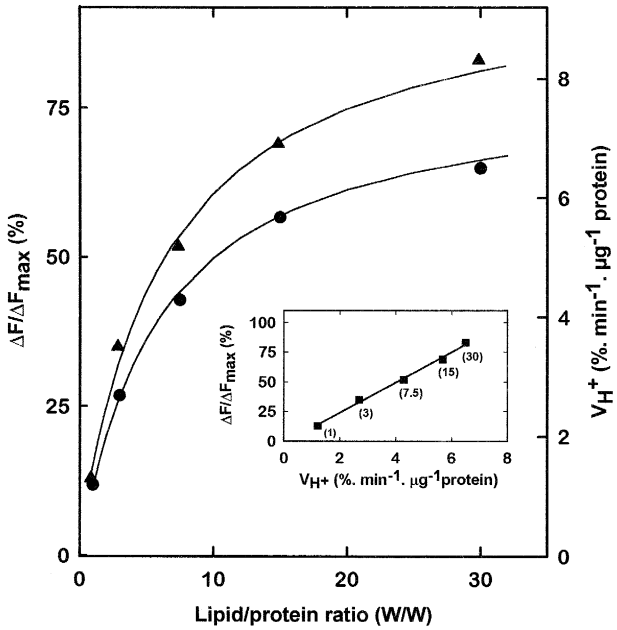

Fig. 2. Effect of the lipid to protein ratio used in protein reconstitution on the electrogenic H^+-pumping activity of the plasma membrane (H^+)ATPase. The membrane potential and the pH gradient were detected using the oxonol and ACMA fluorescent probes, respectively. V_H+: initial rate of ACMA quenching (●); $\Delta F/\Delta F_{max}$: response of oxonol (▲). ΔF_{max} was the maximum value of ΔF extrapolated from Scatchard plot (*not shown*). Inset: correlation between the oxonol and ACMA responses.

To confirm the absence of plasma membrane (H^+)ATPase latency after reconstitution of protein from microsomes and plasma membrane fraction, proteoliposomes were treated with SDS [16] as described in Section 2. Indeed, a strong increase of the plasma membrane (H^+)ATPase activity in native vesicles was observed after SDS treatments (Fig. 3). These maximum activities were nearly the same as the activities observed in the presence of Triton X-100 for untreated vesicles. After reconstitution of protein from both microsomes and plasma membrane, SDS treatment failed to demask any latent plasma membrane (H^+)ATPase activity.

After reconstitution, whole proteins and lipids comigrated at the same buoyant density on a linear glycerol density gradient, higher than the one of liposomes (Fig. 4), and lower than that of native vesicles which sedimented at the bottom of the gradient (data not shown). This result indicates that a single population of proteoliposomes was obtained after reconstitution of plasma membrane proteins into

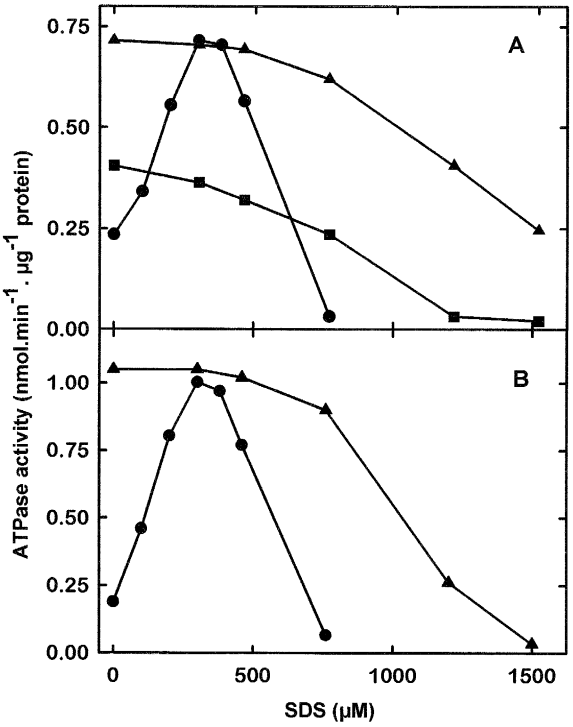

Fig. 3. (H^+)ATPase latency in microsomes and phase-partitioned plasma membranes, before and after reconstitution. (H^+)ATPase latency was determined using SDS treatment as described in Section 2. (A), microsomes: native membranes (●); reconstituted membranes in the absence (■) or in the presence of 20% (v/v) glycerol (▲); (B), phase-partitioned plasma membranes: native membranes (●); reconstituted membranes in the presence of 20% (v/v) glycerol (▲).

fresh lipids at a lipid to protein ratio R = 15 (w/w), as described in Section 2.

3.2. Evidence for a passive NO_3^- transport system coupled to the (H^+)ATPase

Plasma membrane proteins were reconstituted in a buffer containing either 50 mM K_2SO_4 or 50 mM Li_2SO_4 and assayed in a medium containing 50 mM K_2SO_4. In both cases, a negligible H^+-pumping but a large membrane potential were observed after energization of the pump (Fig. 5). This indicated that the active H^+ influx could not be electrically compensated by a cation efflux or an anion influx: the (H^+)ATPase stalled on the high membrane potential it created.

The presence of 100 mM K^+ inside the plasma membrane vesicles failed to generate a sufficient K^+ efflux to compensate the active H^+ influx. Addition of the ionophore valinomycin was necessary to trigger a strongly depolarizing K^+ efflux from the vesicles, enabling a high H^+-pumping rate (Fig. 5A and 5B). The short-circuiting of the H^+-pump by valinomycin was transient, probably because the interior of the vesicles was rapidly depleted in K^+, due to their small size: the H^+-pumping decreased anew, while a high membrane potential was recovered. The latter was totally collapsed by addition of the protonophore FCCP.

In a second experiment (Fig. 5C,D), 20 mM NO_3^- was added, as a concentrated aliquot of BTP-salt, to the outside of the vesicles instead of valinomycin. This addition triggered a high H^+-pumping rate and a stable and nearly complete depolarization of the vesicles. In this experiment, the short-circuiting effect of NO_3^- could be sustained durably since its concentration remained constant outside the vesicles. These results suggest that plasma membrane contains an intrinsic transport system enabling a passive NO_3^- influx (i.e., driven by the membrane potential), capable to fully compensate the active H^+ influx. In the

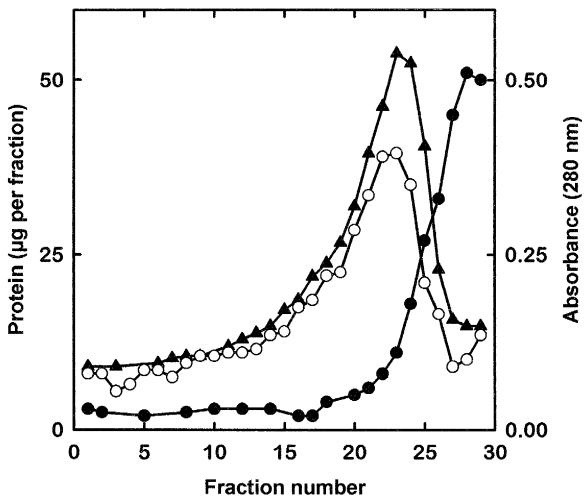

Fig. 4. Distribution of lipids and proteins on a linear glycerol density gradient of the reconstituted vesicles from microsomes. An aliquot of reconstituted proteoliposomes (695 μg protein and 10 mg lipid) or liposomes (10 mg lipid) in reconstitution buffer was applied to a linear glycerol gradient (34 ml, 25% to 50% v/v, in reconstitution buffer), centrifuged for 15 h at 150 000 × g, and fractions (1.5 ml) were collected and assayed for proteins (○), as described in Section 2. The turbidity of the suspension of liposomes (●) and proteoliposomes (▲) was measured at 280 nm.

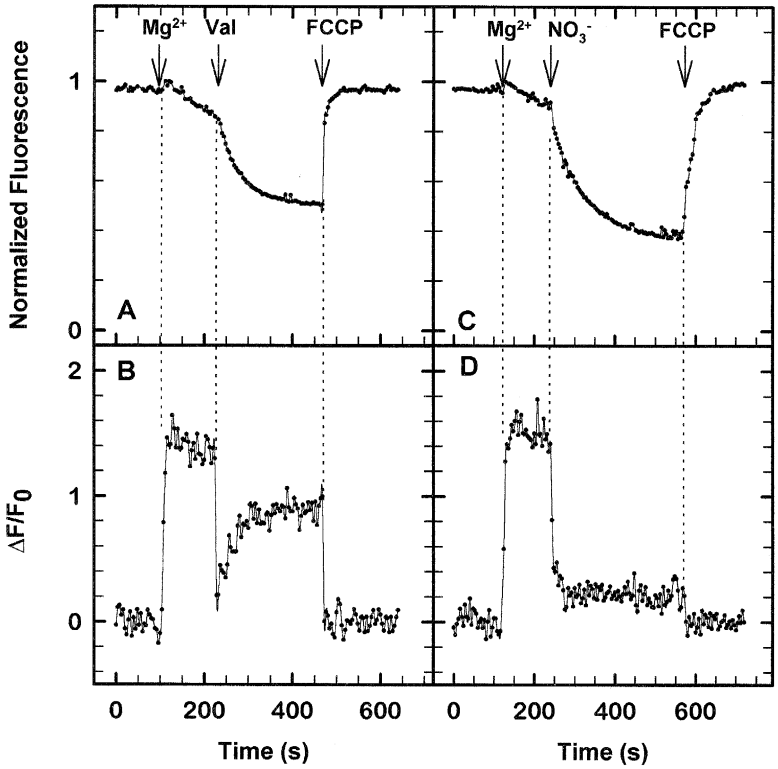

Fig. 5. Nitrate or K^+ electrical short-circuiting of the (H^+)ATPase of reconstituted plasma membrane vesicles. Vesicle acidification and membrane potential were simultaneously monitored with ACMA (in A and C) and oxonol (in B and D) probes, respectively. Reconstitution buffers contained 10 mM BTP-SO_4 (pH 7.5) and 50 mM K_2SO_4 (A and B), or 50 mM Li_2SO_4 (C and D). At the indicated times, Mg^{2+} was added to activate the (H^+)ATPase; NO_3^- (20 mM, BTP salt) or valinomycin (100 nM) to collapse the electrical potential; and FCCP (200 nM) to collapse both pH and electrical gradients.

presence of 20 mM NO_3^-, this system should have a conductance comparable to that induced by valinomycin in the presence of 100 mM K^+.

The H^+-pumping rate could be taken as an estimate of the net influx of NO_3^- since the H^+-pumping was totally dependent on NO_3^- addition. This NO_3^--dependent H^+ pumping was measured as a function of NO_3^- concentration, using three kinds of membrane vesicles preparations: native plasma membrane vesicles, reconstituted vesicles from the whole plasma membrane protein content, and vesicles reconstituted from the solubilized and glycerol gradient purified (H^+)ATPase. The assay medium contained KNO_3 at various concentrations, and K_2SO_4 to make the K^+ final concentration equal to 100 mM.

In the presence of 100 nM valinomycin, the H^+-pumping rate (% quenching $\cdot$ $min^{-1} \cdot \mu g^{-1}$ protein) increased from 0.3 (native plasma membrane) to 5.0 (reconstituted plasma membrane) and to 130 (reconstituted purified (H^+)ATPase), but the H^+-pumping rate of the three vesicle preparations remained insensitive to NO_3^- addition (0 to 50 mM, Fig. 6).

Conversely, in the absence of valinomycin, the H^+-pumping rate of the three vesicle preparations displayed strongly different responses to NO_3^- addition (0–50 mM). The H^+-pumping of both native and reconstituted plasma membrane vesicles increased with NO_3^- concentration according to saturation-like kinetics (Fig. 6A,B), up to the corresponding maximum H^+-pumping rate obtained previously in the presence of valinomycin. The K_m values determined from the Scatchard plots (Fig. 6, insets) were 4.6 mM and 5.1 mM for native and reconstituted plasma membrane vesicles, respectively. No NO_3^- stimulation of the H^+-pumping activity was observed when the solubilized and glycerol gradient purified (H^+)ATPase was assayed in the absence of valinomycin (Fig. 6C). In this case, the H^+-pumping remained 4-fold lower than the one observed in the presence of valinomycin.

The selectivity of the short-circuiting of H^+-pumping by anions (20 mM K^+-salts) was determined on native and reconstituted plasma membrane vesicles. The observed sequence was $NO_3^- > I^- \approx ClO_3^- \approx Br^- > Cl^- \approx NO_2^- > IDA^- \approx SO_4^{2-}$ (Table 2). When reconstituted vesicles were incubated for various times at 30°C, the rate of the H^+-pumping remained constant when the pump was short-circuited by K^+-valinomycin, whereas it decreased following a first order process (time constant of 4–5 h) when the pump was short-circuited by NO_3^- (Fig. 7). Among the various inhibitors tested which did not inhibit the

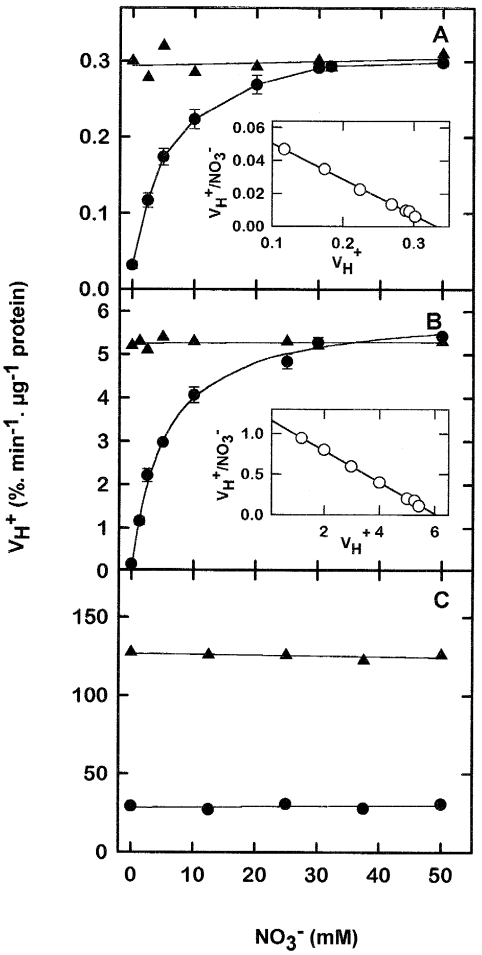

Fig. 6. Response of the initial rate of ATPase H^+-pumping to NO_3^- concentration. The initial rate of ACMA quenching (V_H+) was determined in native (A), or reconstituted (B) plasma membrane vesicles, and in proteoliposomes reconstituted with (H^+)ATPase purified on a glycerol gradient (C). Reconstitution buffer contained 10 mM BTP-SO_4 (pH 7.5) and 50 mM Li_2SO_4 (●), or 50 mM K_2SO_4 (▲). The assay medium contained KNO_3 at the indicated concentration and K_2SO_4 to make the K^+ final concentration up to 100 mM, in the absence (●) or in the presence (▲) of 100 nM valinomycin. The K_m and V_H+_{max} values determined from the Scatchard plots of the NO_3^--dependent H^+-pumping activities (insert) are respectively 4.6 mM and 0.33%·min^{-1}·µg^{-1} protein with native vesicles (A) and 5.1 mM and 6.1%·min^{-1}·µg^{-1} protein with reconstituted plasma membrane vesicles (B).

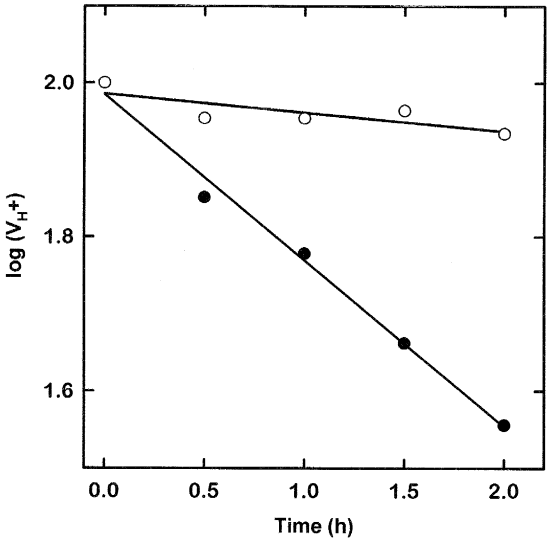

Fig. 7. Effect of ageing on the short-circuiting of (H^+)ATPase by NO_3^-. The initial rate of ACMA quenching (V_H+) was determined in plasma membrane vesicles reconstituted in 10 mM BTP-SO_4 (pH 7.5) and 50 mM Li_2SO_4 (●), or 50 mM K_2SO_4 (○). The assay medium contained 10 mM BTP-SO_4 (pH 6.5), 20 mM KNO_3 and 40 mM K_2SO_4, in the absence (●) or in the presence (○) of 100 nM valinomycin. Proteoliposomes were kept at 30°C in reconstitution buffers for the indicated times.

Table 2
Effect of various anions on the (H^+)ATPase short-circuiting

Anions	Native plasma membrane		Reconstituted plasma membrane	
	V_H+ (% min^{-1} µg^{-1} protein)	% of control	V_H+ (% min^{-1} µg^{-1} protein)	% of control
NO_3^-	0.300	100	6.0	100
I^-	0.234	78	5.0	84
ClO_3^-	0.240	80	4.7	78
Br^-	0.198	66	4.6	77
NO_2^-	0.171	57	3.5	58
Cl^-	0.171	57	3.7	61
SO_4^{2-}	0.060	20	1.5	25
IDA^-	0.075	25	1.5	25

Anions were added as 20 mM K-salts.

Table 3
Effect of inhibitors on K^+-valinomycin and NO_3^--dependent H^+ pumping by (H^+)ATPase

Inhibitors	Protocol	Inhibition (%)	
		K^+-valinomycin	NO_3^-
DEPC	a	93±7	94±8
PGO	a	2±9	65±6
DIDS	a	0±4	6±8
La^{3+} 100 μM	b	76±5	87±7
NPPB 500 μM	b	7±10	5±5
AE 500 μM	b	74±8	90±6
A-9-C 500 μM	b	3±5	5±4

The initial rate of ACMA quenching was determined in the two conditions detailed in the legend to Fig. 7, quoted here as 'K^+-valinomycin' and 'NO_3^-'. Two protocols were used: native vesicles were incubated for 45 min at 6°C in the presence of 12 mM inhibitor before reconstitution (a); proteoliposomes were incubated for 10 min with inhibitor in the measure cuvette before energization of the (H^+)ATPase (b).

(H^+)ATPase, only PGO was efficient to inhibit (65%) NO_3^- dependent short-circuit (Table 3).

3.3. Evidence for a passive NO_3^- transport system using K^+-diffusion gradient in the presence of valinomycin

Reconstituted plasma membrane vesicles, but not native ones, were suitable to sustain high membrane potential in response to imposed K^+ diffusion gradient (100 mM outside, 1 mM inside, as SO_4^{2-} salt) in the presence of valinomycin (Fig. 1C). When the same K^+ concentration gradient was created with 20 mM KNO_3 plus 40 mM K_2SO_4, the maximum fluorescence ratio of the oxonol VI dye was nearly the same as the one in absence of NO_3^-, but its dissipation rate strongly increased (Fig. 8). Only a small increase of the dissipation rate was observed when the same experiment was performed on control liposomes.

The dissipation of the fluorescence ratio of the membrane potential probe evidenced the dissipation of the imposed K^+ gradient. Owing to the large size asymmetry of internal/external compartments, the K^+ concentration outside could be considered as constant. Thus, the dissipation of the K^+ gradient only resulted from the filling of the vesicles and consequently, the dissipation rate of the fluorescence ratio (in $\%.s^{-1}$) could be taken as an estimate of the K^+ net influx facilitated by valinomycin. It is noteworthy that the large stimulation of the K^+ net influx by NO_3^- was observed, whereas both initial maximum ratio of oxonol VI fluorescence (i.e. the initial maximum membrane potential) and valinomycin concentration were the same, independently of the presence of NO_3^-. This indicated that the net K^+ influx was actually restricted by the size of the electrically compensating ion leak, and not by the conductance of membrane vesicles conferred by valinomycin. This was confirmed by the instantaneous dissipation of the membrane potential (i.e., of the K^+ gradient) upon addition of the Li^+ ionophore ETH (or protonophore FCCP, data not shown). This demonstrates that valinomycin could promote very large K^+ influx capable to fill instantaneously the vesicles, provided that a large compensating Li^+ efflux from membrane vesicles containing 0.1 M Li^+ was facilitated by ETH addition.

In summary, it could be assumed that: (1) the dissipation rate of the fluorescence ratio gave a quantitative estimate (expressed as $\%.s^{-1}$) of the net K^+

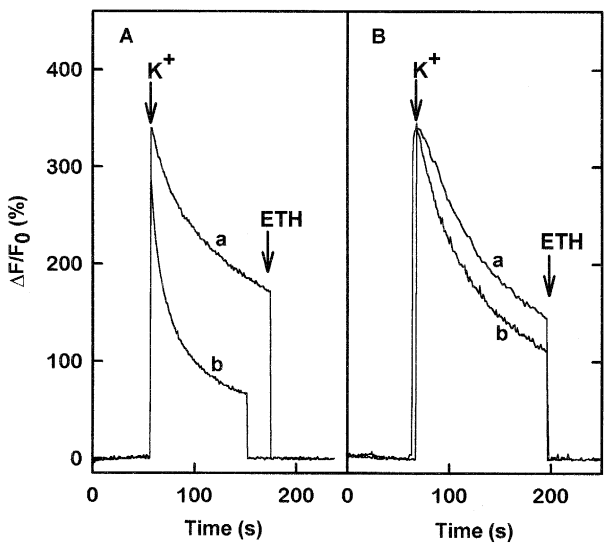

Fig. 8. Effect of NO_3^- on the dissipation of K^+-valinomycin diffusion potential across reconstituted plasma membrane vesicles or liposomes. Membrane potential across reconstituted plasma membrane vesicles (A, 3.4 $\mu g \cdot ml^{-1}$ protein with 50 $\mu g \cdot ml^{-1}$ lipids), or control liposomes (B, 50 $\mu g \cdot ml^{-1}$ lipids) was monitored with oxonol. Vesicles were polarized by addition of K_2SO_4 (traces a), or K_2SO_4 *plus* KNO_3 (traces b) in the presence of 20 nM valinomycin. Final concentrations of K^+ and NO_3^- were 100 mM and 20 mM, respectively. The Li^+ ionophore ETH (200 nM) was added to collapse the membrane potential.

influx facilitated by valinomycin; (2) the dissipation rate of the fluorescence ratio was actually restricted by the intensity of the ion leaks electrically neutralizing the net K^+ influx, and thus could be actually considered as a quantitative estimate of these ion fluxes.

We demonstrated previously [20] in similar experiments with liposomes multilabelled with fluorescent probes, specific for H^+ and K^+, that H^+ was the only ion species which significantly contributed to the ion leak, in the absence of NO_3^-. Thus, ion leak in the presence of NO_3^- arose from both net H^+ and NO_3^- fluxes. As habitual in electrophysiological analysis of ion currents, the net NO_3^- influx was extracted in the following as the difference between the initial dissipation rates of the oxonol VI fluorescence ratio in the presence and in the absence of NO_3^- ($V_{NO_3^-}$, in $\%.s^{-1}$).

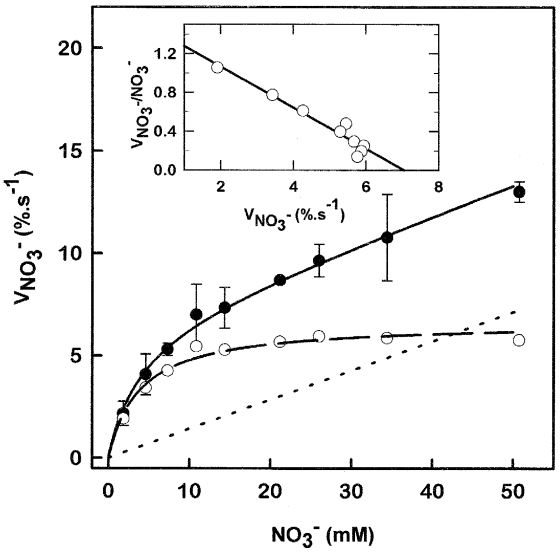

Fig. 9. Effect of NO_3^- concentration on the initial rate of dissipation of K^+-valinomycin diffusion potential. Reconstituted plasma membrane vesicles were polarized in the presence of valinomycin by addition of 100 mM K^+, as a mixture of SO_4^{2-} and NO_3^- salts at the indicated NO_3^- concentration. The NO_3^--dependent increase of the initial dissipation rate of the oxonol VI fluorescence ratio ($d(\Delta F/F_0)/dt\% \cdot s^{-1}$) was assimilated to the initial rate of NO_3^- transport ($V_{NO_3^-}$). The observed kinetics was interpreted as the sum of a facilitated diffusion, saturable according to Michaelis-Menten relationship, and a non-facilitated diffusion across lipidic bilayer, linear with NO_3^- concentration. The slope of the linear regression of the data obtained at NO_3^- concentrations higher than 25 mM allowed to estimate the non-facilitated component (dashed line, $V = k.[NO_3^-]$, with $k = 0.14\% \cdot s^{-1} \cdot mol^{-1} \cdot m^3$), and then to deduce the facilitated one. Scatchard plot of the latter gave a K_m for NO_3^- of 4.7 mM and a V_{max} of $7.0\% \cdot s^{-1}$ (inset).

$V_{NO_3^-}$ was measured as a function of the NO_3^- concentration added to the exterior of reconstituted plasma membrane vesicles (Fig. 9). The observed kinetics could be fitted by the sum of a first order saturation component plus a linear component. A significant contribution of simple diffusion of NO_3^- across lipidic bilayer could be expected from the NO_3^--dependent increase of the membrane potential dissipation rate observed on control liposomes (Fig. 8B). It is to be noted that the same K^+-gradient was applied in experiments relative to Figs. 8 and 9: indeed, the maximum responses of the probe initially observed, and thus the membrane potential, were nearly the same. On the other hand, only NO_3^- concentration in the outside varied (the interior of the vesicles did not contain NO_3^- initially). The Goldman-Hodgkin-Katz relation predicts that, in such conditions, net ion fluxes are linear with their external concentration [21]. Thus, we hypothesized that the observed linear component corresponded to simple diffusion of NO_3^-, and the saturable one to facilitated NO_3^- transport. The K_m for NO_3^- obtained (4.7 mM) was close to the one obtained from the analysis of the NO_3^--dependent H^+-pumping of the (H^+)ATPase (Fig. 6).

4. Discussion

4.1. Characteristics of native and reconstituted plasma membrane vesicles

Native plasma membrane vesicles have been successfully used to investigate a variety of secondary transports (sugars, amino acids, organic acids, Ca^{2+} [22]). Nevertheless, membrane tightness of native vesicles from maize roots obtained in the present work was not sufficient to sustain imposed diffusion potentials. The decrease of the ratio V_H^+/V_{ATP} (where V_{ATP} is the basal ATP hydrolysis activity) from 5.2 (microsomes) to 2 after plasma membrane purification should result mainly from a decrease of the membrane tightness, since it was reversed after reconstitution of native proteins into fresh lipids (Table 1). This is in agreement with the contention that the tightness to H^+ decreased during membrane isola-

tion, due to time-dependent lipid degradations. Complex lipid degradations induced by cutting and homogenization of plant tissues have been demonstrated even at low temperature [23,24]. Lipid degradations were observed simultaneously to a strong decrease of the H^+-pumping activity of the plasma membrane (H^+)ATPase, after a few hours ageing at 0°C of microsomes from corn root [13]. Thus, it was necessary to develop optimal procedures for the reconstitution of native plasma membrane proteins.

The simple and reliable reconstitution procedure described here gives an homogeneous preparation of highly tight vesicles suitable for studying transport of small mobile ions such as NO_3^-. As discussed in the next section, it permitted to recover several NO_3^- transport properties of the original (native) plasma membrane vesicles (K_m for NO_3^-, anion selectivity).

Homogeneity of reconstituted vesicle population was appreciated first from the (H^+)ATPase sidedness. The latency of the hydrolytic activity of the (H^+)ATPase of native plasma membrane vesicles disappeared after reconstitution (Table 1). Addition of 20% (v/v) glycerol to the reconstitution buffer, a well-known protecting agent, allowed to fully recover the total (H^+)ATPase activity of the native preparation. It could be concluded that the reconstitution step only modified the orientation of (H^+)ATPase, ensuring its unidirectional inside-out reinsertion. A scrambling of proteins is generally observed from reconstitution methods which make use of detergents [25]. On the other hand, similar unidirectional reinsertion of the purified (H^+)ATPase was previously obtained in the absence of detergent [26], provided that preformed lipidic bilayer exhibits hydrophobic defects ('bulging defects') [27]. Unidirectional orientation of a variety of membrane proteins could be obtained using this so-called spontaneous insertion method and was attributed to the large asymmetry of their structure [28]. The cytoplasmic face of the plasma membrane (H^+)ATPase involves about 70% of the primary amino acid sequence [29], and should explain its inside-out orientation after spontaneous reinsertion.

The mechanism explaining the unidirectional inside-out reinsertion of the (H^+)ATPase presently observed with a detergent elimination method could be similar to that reported for reconstitution of bacteriorhodopsin [30]. Upon rapid detergent elimination, lipids reassembly should occur before the spontaneous reinsertion of proteins into the lipidic bilayer, destabilized by high levels of detergent.

The analysis of the buoyant density of reconstituted plasma membrane vesicles in a glycerol gradient allows to verify that the reconstituted fraction only contained proteoliposomes and not a mixture of liposomes and proteoliposomes (Fig. 4). Finally, besides the augmentation of the size and stability of the diffusion membrane potential (Fig. 1C), the increase of the $V_H + /V_{ATP}$ ratio ascertains the improvement of the vesicle tightness after reconstitution.

In summary, the observed increase of the H^+ electrochemical gradient generated by the plasma membrane (H^+)ATPase after proteins reconstitution resulted from both an improvement of membrane tightness and ATP accessibility to the enzymic cytoplasmic catalytic sites. Consequently, the specific H^+-pumping activity increased 5-fold and 20-fold after reconstitution of microsomal and phase-partitioned plasma membrane fraction, respectively (Table 1). The higher augmentation observed with purified plasma membrane can be explained by its lower proportion of inside-out vesicles and its lower membrane tightness. We previously showed that a Triton X-100 washing of phase-partitioned plasma membrane allowed a 10-fold increase of the specific H^+-pumping activity due to partial reorientation of the (H^+)ATPase (from 15% to 50% of inside-out (H^+)ATPase), and to a 65% protein loss [10]. Although Triton X-100 washing treatments were successfully used to study Ca^{2+} transport systems [31], the present reconstitution procedure ensures a complete accessibility to the catalytic site of the (H^+)ATPase without protein loss.

4.2. Assay of passive NO_3^- transport on isolated membrane vesicles

In the present paper, two in vitro transport assays have been set up to study passive NO_3^- transport systems. The first transport assay made use of the interaction between NO_3^- and the electrochemical H^+ gradient built by the plant plasma membrane (H^+)ATPase, and was applicable to both native and reconstituted plasma membrane vesicles. Dissipation by various substrates (ions, sugars, amino acids and organic acids) of the transmembrane pH gradient

pre-established by H^+-pumps has been widely used to identify many secondary active plant H^+: X co-transports [22]. But, as shown in Fig. 5, the initial formation of a pH gradient by the H^+-pump clearly necessitates that the net active H^+ influx should be electrically counterbalanced either by an equivalent net passive efflux of cation (for example, K^+ in the presence of valinomycin, Fig. 5A,B), or a net passive influx of anion (for example, NO_3^-, Fig. 5C,D). Such an approach has previously been used by Kaestner and Sze [32] to investigate passive anion transport in tonoplast vesicles: large-scale quenching of oxonol V dye upon (H^+)ATPase electrical stalling facilitated the kinetic study of its dissipation by subsequent addition of permeant anions. In the present study, we found the use of the most permeant oxonol VI dye most suitable with the simultaneous monitoring of the net active H^+-influx, using the ACMA probe, which depends on the membrane potential relaxation by the addition of permeant anions. Addition of 20 mM NO_3^- to the outside of plasma membrane vesicles triggered a high H^+-pumping associated to a complete depolarization of the vesicles. Since the H^+-pumping was negligible in the absence of NO_3^-, the value of the net passive NO_3^- influx could be estimated by the initial rate of quenching in the presence of NO_3^-.

Several lines of evidence indicate that the net passive NO_3^- influx given by this transport assay was not due to a simple diffusion across lipidic bilayer, but was actually mediated by transport proteins: (1) H^+-pumping activity of the glycerol gradient purified H^+-ATPase, reconstituted in fresh lipids, was insensitive to NO_3^- (Fig. 6C); (2) it was stimulated by NO_3^- in both native and reconstituted plasma membrane vesicles, and the NO_3^--dependent pumping rate was saturable (Fig. 6A,B); (3) this latter decreased upon incubation at 30°C according to a first order kinetics, whereas the K^+-valinomycin dependent pumping rate remained constant (Fig. 7); (4) similarly, the NO_3^--dependent H^+-pumping was inhibited by PGO, and not the K^+-valinomycin dependent one (Table 3).

This transport assay gives limited access to the intrinsic properties of the NO_3^- carrier (e.g., sensitivity to inhibitors or ionic conditions). The ability of NO_3^- to short-circuit the H^+-ATPase (Fig. 5C,D) suggested that interaction of NO_3^- and an imposed diffusion potential could be suitable to detect a passive NO_3^- transport (driven by the membrane potential).

Only reconstituted vesicles could sustain large K^+-valinomycin diffusion potentials because of their higher membrane tightness (Fig. 1C). Since several original NO_3^- transport properties (K_m, selectivity) observed in the native plasma membrane fraction using the previously discussed assay transport, were recovered on reconstituted vesicles, these latter appeared suitable to examine passive NO_3^- transport using imposed diffusion potentials. As detailed in Section 3, the dissipation rate of the imposed diffusion potential only depended on the magnitude of passive H^+ efflux in a medium containing only impermeant ionic species, and of the magnitude of H^+ efflux *plus* NO_3^- influx in NO_3^- containing medium. The value of the K_m for NO_3^- obtained from this second transport assay was similar to the previous one (Figs. 6 and 9). This makes likely that the two different transport assays gave access to the same passive NO_3^- transport system. Analysis of the interaction of NO_3^- and the oxonol VI response to imposed diffusion gradient is currently under progress to determine quantitatively membrane potential and NO_3^- flux. This method will be useful in future studies aiming at the continuation of the functional characterization as well as at the purification and identification of the NO_3^- transport system.

4.3. Main properties of in vitro passive NO_3^- transport

The first transport assay demonstrated the ability of NO_3^- to almost totally short-circuit the (H^+)ATPase (Fig. 5), triggering the vesicle acidification in native or reconstituted plasma membrane vesicles, but not in reconstituted vesicles with purified (H^+)ATPase (Fig. 6). Simple Michaelis kinetics with similar K_m (≈ 5 mM) were observed in the two former cases. From these data, it can be inferred that the short-circuiting by NO_3^- which triggered the H^+-pumping resulted from a secondary transport system mediating a passive NO_3^- influx in the vesicles.

It should be pointed out that both right-side-out and inside-out vesicles were present in native preparations of plasma membrane [10,15] and that only the latter were activated by Mg-ATP. Therefore, the passive NO_3^- transport system demonstrated here in

vitro should mediate a NO_3^- efflux in situ. Nevertheless, most of the data presented in the present paper were obtained using reconstituted plasma membrane vesicles. Nitrate was always added to the outside media to trigger an anion influx into membrane vesicles positively polarized either by the (H^+)ATPase or by an inward K^+ diffusion gradient in the presence of valinomycin. Thus, the orientation of the NO_3^- carrier after reconstitution is to be considered.

Unfortunately, latency of the activity of ion pumps, which is a convenient way to estimate the molecular orientation of ion pumps from their hydrolytic activity [15,16], is not usable for secondary transport systems. Until these latter are characterized at the biochemical level, direct experimental data regarding their orientation is very limited. Therefore, no direct conclusion can be made from the present data about the molecular orientation of the passive NO_3^- transport system.

Indeed, K_m for NO_3^- of reconstituted plasma membrane vesicles, determined with both transport assays (Fig. 6B and Fig. 9), was the same as that for native vesicles (Fig. 6A). This might reflect a scrambled orientation of the NO_3^- carrier in reconstituted vesicles, with its cytoplasmic and extracellular faces displaying the same affinity for NO_3^- (symmetrical carrier). Nevertheless, the observed K_m value (≈ 5 mM) was compatible with reported estimates of cytoplasmic NO_3^- activity [33] and not with usual NO_3^- concentration in external media. Thus, a selective activation by external NO_3^- of the inside-out oriented carrier molecules, present in the mixture of orientations would be a more reasonable hypothesis (irreversible carrier).

Alternatively, all NO_3^- carrier molecules could be inside-out oriented in reconstituted vesicles. Measurement of the latency of the (H^+)ATPase hydrolytic activity in reconstituted plasma membrane vesicles showed that all the enzyme molecules were reinserted according to an inside-out orientation (Fig. 3 and Table 1). As discussed in Section 1, this is probably due to the structural asymmetry of this enzyme. Since most of the transport systems identified so far also exhibit large structural asymmetry in favour of their cytoplasmic face [29,34–37], inside-out unidirectional reinsertion of both (H^+)ATPase and NO_3^- carrier molecules remains finally the most likely hypothesis.

The anionic selectivity observed in vitro on plasma membrane vesicles (Table 2) is not likely to be related to a single transporter but merely reflects the contribution of different anion transport systems on this membrane. Indeed, differences in Cl^-: NO_3^- selectivity of the plasma membrane have been observed between two maize varieties [38]; several studies indicate that NO_3^- and Cl^- conductance probably involve different transport systems of the plasma membrane (reviewed in Ref. [39]).

Conversely, simple Michaelis kinetics with similar K_m values for NO_3^- were observed from both transport assays on reconstituted vesicles (Fig. 6B and Fig. 9), in agreement with that obtained on native vesicles (Fig. 6A). The present data do not allow the determination of whether the observed passive NO_3^- transport results from one or more molecular species of carrier. Nevertheless, it can be operationally referred to as a single kind of carrier with a low affinity ($K_m \approx 5$ mM), with an arginine residue in the transport site as indicated by the total inhibition by PGO, and which is insensitive to DIDS and DEPC (reagents of lysine and histidine residues, respectively) (Table 3).

The observed K_m value in the range of the NO_3^- concentration reported for the cytoplasm of plant root cells [33], favours the physiological implication of this transport system in root cells NO_3^- efflux. The existence of channels allowing anion (NO_3^- and Cl^-) influx at high external anion concentration have been demonstrated by patch clamp measurements on wheat root protoplasts [40,41]. However, these studies provide no evidence for an outward anion channel (allowing anion efflux). Therefore, the transport system described here, which provides a high NO_3^- conductance through the plasma membrane of corn root cells may be the pathway for anion (NO_3^-) efflux. It is as efficient, when functioning at V_{max} (at 20 mM NO_3^-), as valinomycin plus 100 mM K^+ to short-circuit the H^+ current of the (H^+)ATPase.

It is noteworthy that, in various stress conditions (mechanical perturbation and root excision, [42,43]), NO_3^- efflux may overcome influx, leading to an excretion of NO_3^- from root cells. To our knowledge, no anion efflux channel have been characterized in root cortical cells. Slow anion channels permeable to Cl^- and NO_3^- have been demonstrated in isolated xylem parenchyma cells from roots, leading to the

hypothesis that xylem vessels could be passively salt loaded [5]. Further work will be needed to elucidate the physiological role of the passive NO_3^- transport described here.

References

[1] King, B.J., Siddiqui M.Y., Ruth, T.J., Warner, R.L. and Glass, D.M. (1993) Plant Physiol. 102, 1279–1286.
[2] Deane-Drumond, C.E. and Glass A.D.M. (1983) Plant Physiol. 73, 100–104.
[3] Deane-Drumond C.E. (1985) Plant, Cell and Environment 8, 105–110.
[4] Tourraine, B., Clarkson D.T. and Muller B. (1994) In A Whole Plant Perpective on Carbon-Nitrogen Interactions (Roy, J. and Garnier, E., eds.), pp. 11–30, SPB Academic publishing, The Hague.
[5] Wegner, L.H. and Raschke, K. (1994) Plant Physiol. 105, 799–813.
[6] Lu, Q. and Briskin, D.P. (1993) Phytochemistry 33, 1–8.
[7] Siddiqui, M.Y., King, B.J. and Glass, A.D.M. (1992) Plant Physiol. 100, 644–650.
[8] Gibrat, R., Grouzis, J.-P., Rigaud, J., Galtier, N. and Grignon C. (1989) Biochim. Biophys. Acta 979, 46–52.
[9] De Michelis, M.I. and Spanswick, R.M. (1986) Plant Physiol. 81, 542–547.
[10] Galtier, N., Belver, A., Gibrat, R., Grouzis, J.-P., Rigaud, J. and Grignon, C. (1988) Plant Physiol. 87, 491–497.
[11] Grouzis, J.-P., Gibrat, R., Rigaud. J., Ageorges A. and Grignon, C. (1990) Plant Physiol. 93, 1175–1182.
[12] Gibrat, R., Grouzis, J.-P., Rigaud, J. and Grignon C. (1990) Plant Physiol. 93, 1183–1189.
[13] Brauer, D., Hsu, A.F. and Tu, S.I. (1988) Plant Physiol. 87, 598–602.
[14] Ames, B.N. (1966) Methods Enzymol. 8, 115–118.
[15] Grouzis, J.-P., Gibrat, R., Rigaud, J. and Grignon, C. (1987) Biochim. Biophys. Acta 903, 449–464.
[16] Palmgren, M.G. and Sommarin, M. (1989) Plant Physiol. 90, 1009–1114.
[17] Ros, R., Romieu, C., Gibrat, R. and Grignon, C. (1995) J. Biol. Chem. 270, 4368–4374.
[18] Schaffner, W. and Weissmann, C. (1973) Anal. Biochem. 56, 502–514.
[19] Larsson, C., Kjellbom, P., Widell, S. and Lundborg, T. (1984) FEBS Lett. 171, 271–276.
[20] Venema, K., Gibrat, R., Grouzis, J.-P. and Grignon, C. (1993) Biochim. Biophys. Acta 1146, 87–96
[21] Hille, B. (1992) In Ionic Channels of Excitable Membranes (Hille, B., ed.), pp. 337–361, Sinauer Associates, Sunderland, MA.
[22] Sze, H. (1985) Ann. Rev. Plant Physiol. 36, 175–208.
[23] Moreau, R.A. (1986) Plant Science 47, 1–9.
[24] Theologis, A. and Laties, G.G. (1981) Plant Physiol. 68, 53–58.
[25] Eytan, G.D. (1982) Biochim. Biophys. Acta 694, 185–202.
[26] Simon-Plas, F., Venema, K., Grouzis, J. -P., Gibrat, R., Rigaud, J. and Grignon, C. (1991) J. Membr. Biol. 120, 51–58.
[27] Chernomordik, L.V., Melikian, G.B. and Chimadzhev, Y.A. (1987) Biochim. Biophys. Acta 906, 309–352.
[28] Jain, M.K. and Zakim, D. (1987) Biochim. Biophys. Acta 906, 33–68.
[29] Serrano, R. (1989) Annu. Rev. Plant Physiol. Plant Mol. Biol. 40, 61–94.
[30] Rigaud, J.L., Paternostre, M.T. and Bluzat, A. (1988) Biochemistry 27, 2677–2688.
[31] Kasai, M. and Muto, S. (1990) J. Membrane. Biol. 114, 133–190.
[32] Kaestner, K.H. and Sze, H. (1987) Plant Physiol. 83, 483–489.
[33] Miller, A.J. and Smith, S.J. (1992) Planta 187, 554–557.
[34] Anderson, J.A., Huprikar, S.S., Kochian, L.V., Lucas, W.J. and Gaber, R.F. (1992) Proc. Natl. Acad. Sci. 89, 3736–3740.
[35] Sentenac, H., Bonneaud, N., Minet, M., Lacroute, F., Salmon, J.M., Gaymard, F. and Grignon, C. (1992) Science 255, 663–665.
[36] Cao, Y., Ward, J.M., Kelly, W.B., Ichida, A.M., Gaber, R.F., Anderson, J.A., Uozumi, N., Schroeder, J.I. and Crawford, N.M. (1995) Plant Physiol. 109, 1093–1106.
[37] Kopito, R.R. and Lodish, H.F. (1985) Nature 316, 234–238
[38] Fischer-Schliebs, E., Varanini, Z. and Lüttge, U. (1994) J. Plant Physiol. 44, 505–512.
[39] Kleinhofs, A. and Warner, R.L. (1990) In The Biochemistry of Plants: A Comprehensive Treatise (Miflin, B.J. and Lea, P.J., eds.), Vol. 16, pp. 89–120, Academic Press, San Diego.
[40] Skerrett, M. and Tyerman, S.D. (1994) Planta 192, 295–305.
[41] Garrill, A., Tyerman, S.D., Findlay, G.P. and Ryan, P.R. (1996) Aust. J. Plant Physiol. 23, 527–534.
[42] Macduff, J.H. and Jacksson, S.B. (1992) J. Exp. Bot. 43, 525–535.
[43] Pearson, C.J., Volk, R.J. and Jacksson, W.A. (1981) Planta 152, 319–327.